JOURNAL OF MATERIALS SCIENCE 18 (1983) 562–570

The role of Coble creep and interface control in superplastic Sn–Pb alloys

J. H. SCHNEIBEL,* P. M. HAZZLEDINE†
Department of Metallurgy and Science of Materials, University of Oxford, Parks Road, Oxford, UK

The creep behaviour of superplastic Sn–2 wt% Pb and Sn–38.1 wt% Pb is investigated at temperatures between 298 and 403 K and for grain sizes between 2.5 and 260 μm. In Sn–2 wt% Pb with grain sizes larger than $\sim$ 50 μm, diffusion-controlled Coble creep is found and it is experimentally shown that this type of creep is inhibited in small-grained specimens. Measurements covering low stresses ($\sim$ 0.1 MPa) and strain rates ($\sim 10^{-10}$ sec^{-1}) rule out any explanation which relies on a threshold stress for plastic deformation. The observations are explained by a model in which, at low stresses or small grain sizes, Coble creep is rate-limited not by diffusion of vacancies but by the rate of emission and absorption at the curved dislocations in the grain boundaries which are the ultimate sources and sinks of vacancies.

1. Introduction

Coble creep [1] has frequently been put forward to explain the mechanical behaviour of superplastic metals and alloys (e.g. [2–5]). One reason for this is the often found strong dependence in superplastic materials of the strain rate, $\dot{\epsilon}$, on the grain size, L (often $\dot{\epsilon}|_{\sigma=\text{const}} \propto L^{-p}$, where σ is the applied stress and p is close to 3, see for example, [6]). Also, in agreement with the occurrence of Coble creep, activation energies of superplastic deformation similar to those of grain-boundary (GB) self-diffusion have frequently been observed [7–9]. However, the measured strain-rate sensitivity of the flow stress, $m = (\partial \log \sigma / \partial \log \dot{\epsilon})|_{T, L=\text{const}}$, where T is the test temperature, is usually below that predicted for Coble creep ($m = 1$). At high stresses this feature can be explained by the onset of power law dislocation climb creep with an m value of $\sim$0.2 [10, 11] but at low stresses the explanation is much less certain. The value of m may be reduced at low stresses by the presence of a threshold stress [2] which implies that below this stress vacancies cannot be created or annihilated at a grain boundary in response to the applied stress [3, 12]. Alternatively vacancies may be created at grain boundaries at such a slow rate that Coble creep ceases to be diffusion-controlled and becomes interface-controlled [12, 13]. In order to detect whether or not the creep is interface-controlled the usual procedure is to calculate Coble creep rates from independently measured GB self-diffusion coefficients and to compare them with the measured creep rate [6, 14]. If the calculated creep rates are higher than the measured ones, Coble creep is concluded to be inhibited by an interface mechanism. The main difficulty with this approach is the low accuracy of experimentally determined GB self-diffusion coefficients. Rather than using these coefficients it is therefore preferable to find direct experimental proof for the existence of Coble creep in superplastic alloys by verifying the characteristic dependence of the strain rate on stress, grain size and temperature. The rate of Coble creep, for a constant applied stress and at a constant temperature, is proportional to $1/L^3$. If the rate of an assumed mechanism inhibiting Coble creep at low stresses varies more weakly than $1/L^3$, e.g. $\dot{\epsilon} \propto 1/L$, and if the stresses are so low that

*Present address: Metals and Ceramics Division, Oak Ridge National Laboratory, P.O. Box X, Oak Ridge, Tennessee, 37830, USA.
†Temporary address: CSIRO Division of Chemical Physics, P.O. Box 160, Clayton, Victoria, Australia 3168.

 0022–2461/83/020562–09$03.58/0

dislocation creep is negligible, an increase in the grain size widens the stress interval in which Coble creep is diffusion-, rather than interface-controlled. The determination of the Coble creep rates for large grain sizes and their extrapolation to small grain sizes then reveals unambiguously the importance of interface processes in the deformation behaviour of small grained materials.

Many superplastic alloys consist of similar volume fractions of two phases and it may be difficult to obtain large equiaxed grains. For this reason a dilute superplastic alloy was preferred for this research. In particular, an Sn–2 wt% Pb alloy was chosen since it can be made superplastic with fairly stable grain sizes as small as 3 μm [15] and as large as 260 μm. In addition, some experiments were done with Sn–38.1 wt% Pb (eutectic composition) which has a more stable grain size than Sn–2 wt% Pb and is therefore particularly suitable for long-term creep experiments at low strain rates.

2. Experimental procedure

Sn–Pb alloys were prepared by melting appropriate proportions of Sn and Pb of 99.999% purity in air (in a few cases in argon) and air-casting into a copper mould with dimensions $10 \times 38 \times 95\,mm^3$. The ingots were rolled down from 10 mm to thicknesses between 0.2 and 1 mm and tensile samples with a gauge length of 26 mm and a width of 6 mm were punched from the rolled sheet. The as-rolled samples were usually stored in liquid air prior to the tests in order to reduce grain growth. Other samples were heat treated in silicone fluid to produce a range of grain sizes. For example, in Sn–38.1 wt% Pb (eutectic composition) heat treatments of 24 h at 433 K and 475 h at 441 K result in mean phase-boundary intercept lengths of 5.9 and 9.9 μm, respectively [16, 17]. In Sn–2 wt% Pb, heat treatments of 900 sec at 393 K and 700 sec at 453 K lead to mean grain-boundary intercept lengths of 35 and 170 μm, respectively. True grain sizes, L, were determined from metallographic cross-sections perpendicular to the tensile axis of the samples as $L = (4/\pi)^{3/2} A_a^{1/2}$ [18] where A_a is the average intersect area of the grains (no distinction was made between phase and grain boundaries). The sample thicknesses were always larger than twice the respective true grain sizes.

Tensile tests at stresses larger than ~ 10 MPa and strain rates in excess of $\sim 10^{-7}\,sec^{-1}$ were performed in silicone fluid in a constant stress creep rig. At low stresses the samples were tested in silicone fluid in a constant load creep rig. Since the elongations employed were only a few percent the stress corresponding to a particular load could be considered as approximately constant. At ~ 300 K the strain resolution and temperature accuracy of the constant load rig were $\pm 10^{-5}$ and ± 0.2 K, respectively. At higher temperatures these values increased to 3×10^{-5} and ± 0.5 K, respectively. For each sample the steady-state strain rates corresponding to many different stresses were determined. At low strain rates (e.g. $< 10^{-8}\,sec^{-1}$) loading periods lasting several days were often required before an approximately constant strain rate could be established. At the lowest strain rates, $\sim 10^{-10}\,sec^{-1}$, a loading period of 3 weeks yielded a maximum strain of only 0.02%. Once a sample had been tested at many different stresses the strain rate corresponding to the initially applied stress was re-measured. Since the strain rate depends strongly on the grain size [2] the approximate agreement found between the strain rates at the beginning and at the end of a test indicated that no significant grain growth had occurred during the test.

3. Experimental results

3.1 Sn–2 wt% Pb

The measured relationship between stress and strain rate for Sn–2 wt% Pb at 298 K is shown in Fig. 1. The measurements agree well with previously published data [15, 19]. When the grain size is small the rate sensitivity is almost constant ($m \simeq 0.45$) over 5 decades of strain rate but for grain sizes of 50 μm and above, a transition is observed between low values of m at high stresses and high values (> 0.5) at low stress. At temperatures higher than 298 K strain-rate sensitivities close to 1 are observed (Fig. 2 and Table I).

The data in Figs. 1 and 2, as well as other data not shown here, have been cross-plotted to obtain the grain-size dependence of the strain rate (Fig. 3) in the region where m is large. At a stress of 1 MPa, corresponding to maximum strain-rate sensitivity, the strain rate is accurately proportional to L^{-3}, indicating that Coble creep is operating.

Also, in the region of high rate sensitivity, the temperature dependence of the strain rate was analysed using the Coble creep equation (which is appropriate for the small strains involved in these experiments):

$$\dot{\epsilon} = \frac{47\Omega w D_0 \sigma}{kTL^3} \exp\left(-\frac{Q_B}{RT}\right), \qquad (1)$$

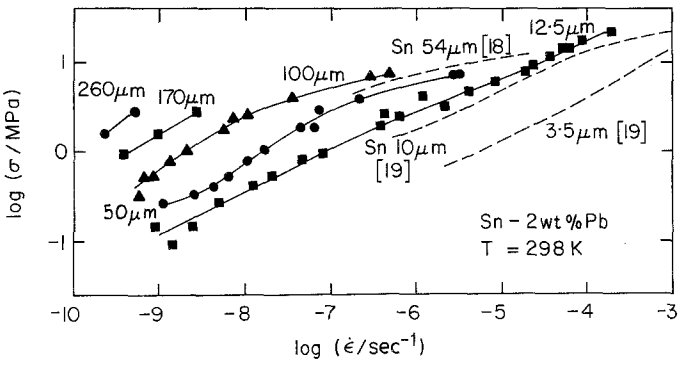

Figure 1 The relationship between the applied stress, σ, and plastic strain rate, $\dot{\epsilon}$, at 298 K for Sn–2 wt% Pb with various grain sizes. Published data for Sn and Sn–2 wt% Pb are included for comparison.

where Ω is the atomic volume, w is the GB width, k is Boltzmann's constant and D_0 and Q_B are the pre-exponential factor and the activation energy for diffusion, respectively. From Equation 1 one obtains:

$$Q_B = -R \left. \frac{\partial \ln (\dot{\epsilon}T)}{\partial (1/T)} \right|_{L,\, \sigma = \text{const}} . \quad (2)$$

From a plot of $\dot{\epsilon}T$ against $1/T$ (Fig. 4) an average activation energy of 42 kJ mol^{-1} is found at a stress of 1 MPa.

Using the measured strain rates and after rearranging Equation 1:

$$D_0 = \frac{\dot{\epsilon} k T L^3}{47 \Omega w \sigma} \exp\left(\frac{Q_B}{RT}\right) . \quad (3)$$

Using $Q_B = 42$ kJ mol^{-1}, $\Omega = 2.7 \times 10^{-29}$ m^3, and $w = 0.7$ nm, D_0 is found to be in the range 2.0×10^{-4} to 3.3×10^{-4} m^2 sec^{-1} with an average value of 2.4×10^{-4} m^2 sec^{-1}.

The best estimate for the GB diffusion coefficient derived from the Coble Creep data is, therefore, 2.4×10^{-4} m^2 sec^{-1} exp (-42 kJ mol^{-1}/RT).

3.2. Sn–38.1 wt% Pb

The relationship between the stress and the strain rate for Sn–38.1 wt% Pb at 298 K and with grain sizes between 2.5 and 20 μm is shown in Fig. 5. The forms of the curves are similar to that for Sn–2 wt% Pb with a grain size of 12.5 μm (Fig. 1). The strain-rate sensitivities vary between 0.34 and 0.52. The strain rates obtained are similar to those obtained by extrapolating the data of Mohamed and Langdon [7], using their grain-size exponents, activation energies and stress exponents. The marked difference in the strain-rate sensitivities found by Mohamed and Langdon in their regions I and II could, however, not be repeated. No evidence for a threshold stress for plastic deformation has been detected although stresses and strain rates as low at 0.1 MPa and 10^{-10} sec^{-1}, respectively, were employed. The threshold stress of 0.18 MPa, found by Burton [21] under similar experimental conditions, could thus not be substantiated. The present results are also quite different from those obtained by stress relaxation testing [22] both in regard to the detection of a threshold stress and to the measurement of m. The reason for this discrepancy is that anelastic effects are important in stress relaxation experiments [23]. However, our results are in qualitative agreement with the observations of Ashby [24] that Pb, with $L = 50$ μm, continues to creep at a measurable rate at very low stresses (~ 0.1 MPa).

In Sn–38.1 wt% Pb at a stress of 1 MPa the strain rate is proportional to $1/L^{2.6}$ and at 0.1 MPa

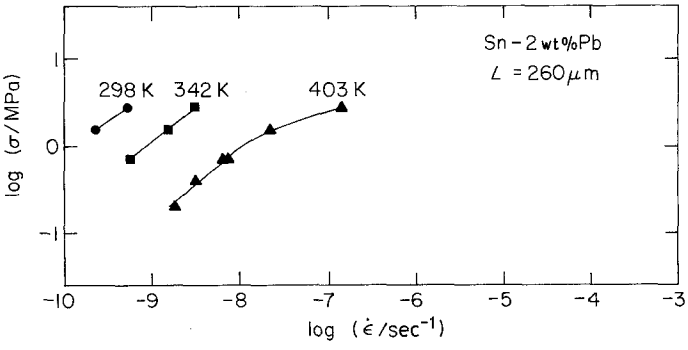

Figure 2 The relationship between the applied stress, σ, and the plastic strain rate, $\dot{\epsilon}$, for Sn–2 wt% Pb with a grain size of 260 μm.

TABLE I Strain-rate sensitivities, m, for Sn–2 wt% Pb for various grain sizes, L, and temperatures, T, at a stress of 1 MPa

	L (μm)								
	12.5	50	50	100	100	170	260	260	260
T (K)	298	298	343	298	343	298	298	343	403
m	0.45	0.68	0.72	0.67	0.68	0.56	0.76	0.82	0.84

this dependence drops to $1/L^2$. Allowing for experimental scatter these results are compatible with the data of Mohamed and Langdon [7] ($\dot{\epsilon} \propto 1/L^{2.3}$). Using the data depicted in Fig. 5 and other data not shown here, an activation energy for the flow of superplastic Sn–38.1 wt% Pb was determined. The analysis of Mohamed and Langdon was employed but using a temperature dependence of the shear modulus (in the range 298 to 423 K) slightly different from theirs [25]. For stresses of 4 and 0.63 MPa, activation energies varying between 46 and 62 kJ mol^{-1} were obtained, with an average value of 55 kJ mol^{-1}. This is substantially in agreement with the results of Mohamed and Langdon (57 kJ mol^{-1}) for their region II. However, as in the case of the rate sensitivity, no clear distinction between region I (low stress) and region II could be found.

4. Discussion

4.1. Coble creep in Sn–2 wt% Pb

The fact that the strain rate is proportional to L^{-3} when the grain size is $> 50\,\mu$m and the stress is ~ 1 MPa strongly suggests that Coble creep operates in these conditions. This conclusion can be strengthened by considering the value of the diffusion coefficient which was measured to be $D = 2.4 \times 10^{-4}$ m^2 sec^{-1} exp $(-42\,\text{kJ mol}^{-1}/RT)$. For comparison [26], the grain-boundary diffusion coefficient of Sn is $D_B = 6.4 \times 10^{-6}$ m^2 sec^{-1} exp $(-40\,\text{kJ mol}^{-1}/RT)$. The bulk self-diffusion coefficients of Sn [26] is $D_L = 7.8 \times 10^{-5}$ m^2 sec^{-1} exp $(-95.5\,\text{kJ mol}^{-1}/RT)$ which agrees closely with the diffusion coefficient of deformation at high stress [27]. The values of the diffusion coefficients may be used to rule out Nabarro–Herring [28] creep as a possible mechanism since the latter will only be faster than Coble creep if $\pi w D_B/LD_L < 1$. The smallest value of this quantity is found for the largest grain size and the largest temperature employed in the experiments ($L = 260\,\mu$m, $T = 403$ K) and it then takes the value 226. Coble creep is, therefore, faster than Herring–Nabarro creep in all our experiments. The difference between the measured diffusion coefficient, D, and the grain-boundary diffusion coefficient of Sn, D_B, is presumably caused by the presence of 2 wt% Pb which may segregate to the

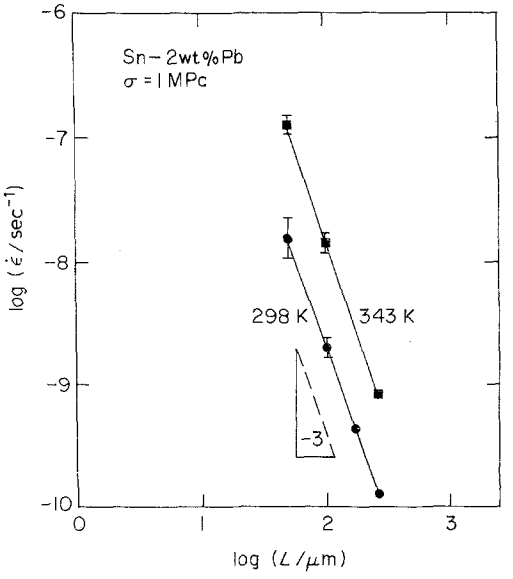

Figure 3 The relationship between the plastic strain rate, $\dot{\epsilon}$, and the grain size, L, for Sn–2 wt% Pb. The errors in the strain rates were estimated from the scatter in the plastic strain rates.

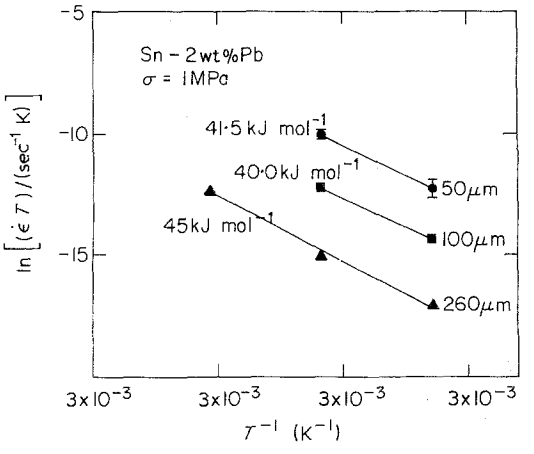

Figure 4 Determination of the activation energy of Sn–2 wt% Pb at a stress of 1 MPa. The error bars were estimated from the scatter in the plastic strain rates.

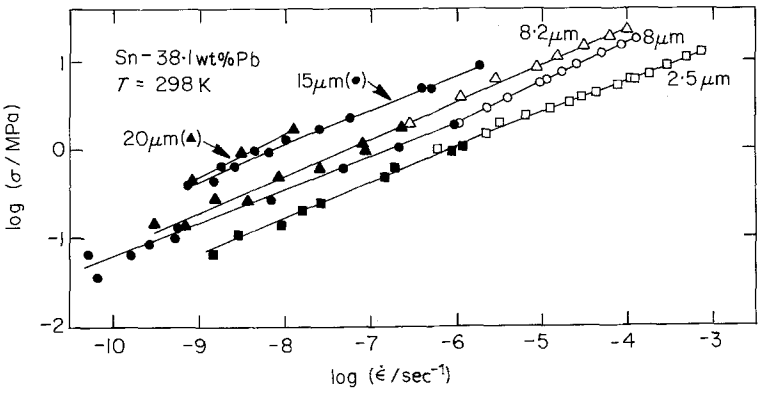

Figure 5 The plastic deformation behaviour of Sn–38.1 wt% Pb at a temperature of 298 K for various grain sizes. Open points, constant stress; closed points, constant load.

grain boundaries. It is interesting to note that the data of Alden [20] on Sn–5 wt% Bi indicate that Bi, like Pb, accelerates grain-boundary diffusion. His alloy also displayed an L^{-3} grain-size dependence of the strain rate and a value of m close to 1. Using his data point, $\sigma = 3.4$ MPa, $\dot{\epsilon} = 1.7 \times 10^{-7}\,\text{sec}^{-1}$, $L = 24\,\mu\text{m}$ (16 μm intercept length), $T = 294$ K and assuming $Q_B = 42\,\text{kJ mol}^{-1}$, the value of D_B(Sn–5 wt% Bi) was found to be $8.8 \times 10^{-5}\,\text{m}^2\,\text{sec}^{-1}\,\exp(-42\,\text{kJ mol}^{-1}/RT)$ which, like D, is considerably larger than the tracer value.

When the grain size is large and the temperature is high, Sn–2 wt% Pb deforms by Coble creep and the deformation parameters determined under these conditions may be used to predict the behaviour at lower temperatures and grain sizes. In Fig. 6, the predicted Coble lines are compared with experiment for $T = 298$ K and $L = 100$, 50 and 12.5 μm. The disagreement between experiment and the Coble line at high stress (~ 10 MPa) is well known to be caused by the onset of power law creep [11], in the case of Sn with an m value of 0.15 [27]. but the disagreement at low stress is less well understood. The effect, however, is a strong one; for $L = 12.5\,\mu\text{m}$ at $\sigma = 10^5$ Pa the actual creep rate is lower than the Coble creep rate by a factor of 100.

It seems likely that Coble creep is also inhibited in Sn–38.1 wt% Pb. The measured strain-rate sensitivities in this material are well below 1 and often smaller than 0.5. The GB diffusivities in Sn and Pb are similar at 298 K (6.4×10^{-13} and $5.3 \times 10^{-12}\,\text{m}^2\,\text{sec}^{-1}$ [29], respectively) so the predicted Coble creep line for $L = 12.5\,\mu\text{m}$ will be closer to its position on Fig. 6. Comparison with Fig. 5 shows again that the measured strain rates at low stresses are much slower than Coble creep would be.

Attempts have been made to explain the inhibition of Coble creep by introducing a threshold stress [3] below which Coble creep ceases to operate. A threshold stress causes a reduction in the strain-rate sensitivity for diffusion creep from $m = 1$ to $m = 0$ in an interval of approximately two decades in the strain rate and approximately one decade in the stress [3, 4]. Neither Sn–2 wt% Pb (with $L = 2.5\,\mu\text{m}$) nor Sn–38.1 wt% Pb display such behaviour; the strain-rate sensitivity remains approximately constant over 5 decades in the strain rate. Threshold stresses arising from GB tension [3] or from the line ten-

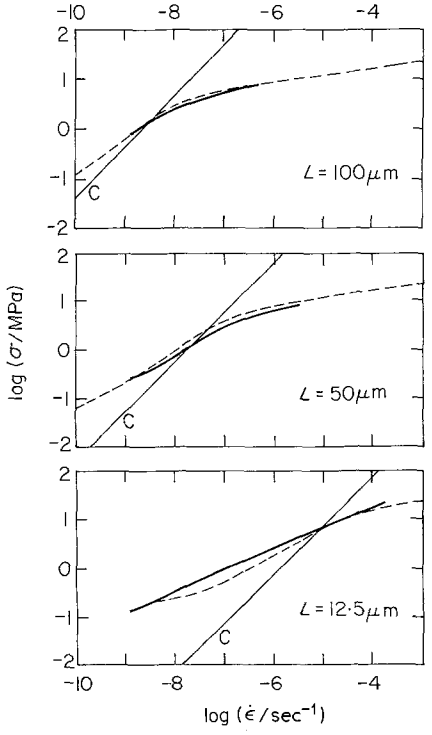

Figure 6 Plastic strain rate as a function of stress: solid line, experiment; broken line, theory; C = Coble creep line; $T = 298$ K.

sion of GB dislocations [30] are proportional to L^{-1} but, for a given strain rate, the stress to deform an alloy is proportional to L^3. The curves of $\ln \sigma$ against $\ln \dot{\epsilon}$ of two specimens of different grain size must, therefore, cross over at some point if a threshold exists. No such behaviour has been observed and we conclude that there is no experimental evidence for a threshold but that if it exists it must be below 10^5 Pa for $L = 12.5\,\mu$m.

4.2. Interface-controlled Coble creep

In previous models of superplasticity [2, 4] it has been suggested that the value of m drops at low strain rates when grain-boundary sliding becomes the slowest mechanism operating. In these models sliding is thought of as a separate mechanism which operates at about the same rate as a grain deformation mechanism such as Coble creep. Models of this type are still tenable since the mechanistic details of grain-boundary sliding and the linkage between sliding and grain deformation are not understood. The present model is an alternative in which Coble creep and grain-boundary sliding are inextricably linked by the fact that the motion of the same set of dislocations causes both plating (grain deformation) and sliding.

During Coble creep vacancies flow from grain faces, which are under tension, to grain faces under compression. The most likely sources and sinks for vacancies are secondary grain-boundary dislocations [13]. These dislocations will generally have components of their Burgers vector normal to the boundary and parallel to the boundary and there will be a step in the boundary at the core of the dislocation [31]. When they move in the boundary the three processes of plating, grain-boundary sliding and grain-boundary migration will occur simultaneously. Coble creep requires the former two in appropriate proportions but not migration; in fact, migration would be resisted by strong chemical forces at interphase boundaries. We assume that dislocations with the required Burgers vectors either exist or can readily be created in the boundary during deformation and that the rate of Coble creep is determined by the rate at which these dislocations can climb. If the dislocations are straight and if their climb is diffusion-limited, the classical Coble creep rate equation (Equation 1) results from such a model. If, however, Bardeen–Herring sources operate or if vacancies condense to create dislocation loops [32] which then expand, the rate of growth of the loops is impeded by the line tension of the dislocations.

The simplest model of this type is shown in Fig. 7: a cubic grain of side L is subject to a shear stress, σ, which causes an interstitial loop to form on the tensile face by the emission of vacancies to a vacancy loop growing on the compressive face. The concentration, C, of vacancies close to the interstitial loop is approximately

$$C = C_0[1 + \Omega(\sigma R\boldsymbol{b} - \Gamma)/R\boldsymbol{b}kT],$$

where C_0 is the thermal equilibrium concentration, R the radius of the loop, Γ the line tension of the dislocation, $\boldsymbol{b}$ is Burger's vector and k is Boltzmann's constant. The concentration falls to C_0 at the edge of the grain. Taking the diffusion to be cylindrical, the flux of vacancies, J, in the grain boundary at radius, r, is

$$J = -D_V C_0 \Omega(\sigma R\boldsymbol{b} - \Gamma)/rkTR\boldsymbol{b} \ln (2R/L),$$

where D_V is the vacancy-diffusion coefficient. If w is the width of the grain boundary through which rapid diffusion takes place, the rate of growth of the loops is

$$\frac{dR}{dt} = \frac{-w\boldsymbol{b}(\sigma R\boldsymbol{b} - \Gamma)}{R^2 kT \ln (2R/L)} D_B. \qquad (4)$$

Equation 4 may be integrated as the loops grow from just above their critical radius ($\alpha\Gamma/\sigma\boldsymbol{b}$, where $\alpha > 1$) to their full size of $R = L/2$ to find the time required to plate one atomic layer on each tensile face of the grain. Taking the slowly varying log term to be constant, $A = -\ln (2R/L)$, the time is

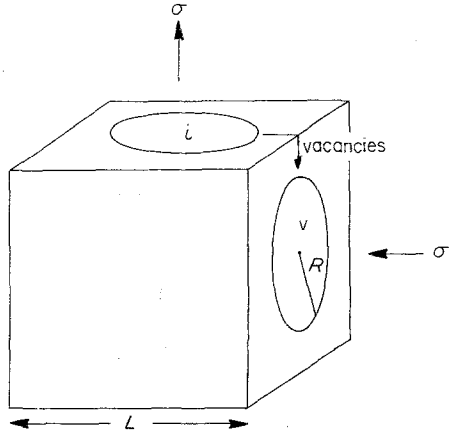

Figure 7 Interface-controlled Coble creep model. Dislocation loops of radius, R, on a grain face of side, L, grow by interchange of vacancies.

$$t = \frac{kTA}{wbD_B}\left\{\frac{L^2}{8\sigma b} + \frac{L\Gamma}{2\sigma^2 b^2} + \frac{\Gamma^2}{\sigma^3 b^3} \times \left[\ln \frac{\sigma bL - 2\Gamma}{2\Gamma(\alpha - 1)} - \frac{\alpha^2}{2} - \alpha\right]\right\}, \quad (5)$$

and in this interval the strain increment $\Delta\epsilon = 2b/L$. The strain rate $\dot{\epsilon} \simeq \Delta\epsilon/t$ may be written in the standard form for sequential operations* [33]:

$$\frac{1}{\dot{\epsilon}_d} = \frac{1}{\dot{\epsilon}_1} + \frac{1}{\dot{\epsilon}_2} + \frac{1}{\dot{\epsilon}_3}$$

where

$$\dot{\epsilon}_1 = 16\sigma D_B b^3 w/(AkTL^3) \quad (6)$$

$$\dot{\epsilon}_2 = 4\sigma^2 b^4 w D_B/(AkT\Gamma L^2) \quad (7)$$

$$\dot{\epsilon}_3 = 2\sigma^3 b^5 w D_B \Big/ \left\{AkT\Gamma^2 L \times \left[\ln \frac{\sigma bL - 2\Gamma}{2\Gamma(\alpha - 1)} - \frac{\alpha^2}{2} - \alpha\right]\right\}. \quad (8)$$

The three terms are recognizable as Coble creep (Equation 6 with $\dot{\epsilon}_1 \propto \sigma/L^3$), Friedel creep [34] (Equation 7 with $\dot{\epsilon}_2 \propto \sigma^2/L^2$) and Nabarro creep [10] modified (see Appendix) in such a way that the climbing dislocations are restricted to move only in grain boundaries (Equation 8 with $\dot{\epsilon}_3 \propto \sigma^3/L$). Because the three creep equations are combined as though there were three sequential operations, it is the slowest which controls the behaviour, the Coble creep may be slowed if either $\dot{\epsilon}_2$ or $\dot{\epsilon}_3$ is less than $\dot{\epsilon}_1$. When $\dot{\epsilon}_1$ is the smallest component of $\dot{\epsilon}_d$ the strain rate is proportional to σ/L^3, the Coble result. When $\dot{\epsilon}_2$ is the slowest component, "Friedel" creep would be observed with an m value of 0.5, and it should be noted that this form of creep equation need not indicate the climb of a dislocation from the head of a pile up. When $\dot{\epsilon}_2$ and $\dot{\epsilon}_3$ are comparable and less than $\dot{\epsilon}_1$, an m value of less than 0.5 would be observed and there would be no simple power law for the grain-size dependence of the strain rate.

Equations 6 to 8 were evaluated using the following values: $D_B = 1.0 \times 10^{-11}\,m^2\,sec^{-1}$, $G = 15.4\,GPa$ [25], $b = 3.5 \times 10^{-10}\,m$, $w = 3b$, $\Gamma = Gb^2/4$, $\alpha = 1.001$, $A = 1$ to give the total rate for diffusive creep in Sn–2 wt% Pb as a function of stress and grain size at 298 K. The value chosen for Γ is lower than normal because the Burgers vectors of the secondary grain-boundary dislocations are likely to be smaller than lattice Burgers vectors. The value of α only affects $\dot{\epsilon}_3^{-1}$ which is a measure of the time required for the loops either to be nucleated (which may be a possible process if b is small [32]) or for climb sources to operate. The model is too simplified to take account of this process properly and the early stages of the formation of a loop are merely simulated here by the use of the parameter α. A detailed model should consider the kinetics of nucleation and should avoid the use of a threshold stress $2\Gamma/bL$ which is built into the simple model but which is not observed in practice.

The full mechanical response is obtained by adding to $\dot{\epsilon}_d$ a power-law creep rate $\dot{\epsilon}_w = 5 \times 10^{15}(\sigma/G)^{6.6}$ obtained by extrapolating the experimental measurements at 402 K of Mohamed *et al.* [27] on Sn. The theoretical line is compared with experiment in Fig. 6 and with the Coble line, Equation 1. The model fits the experimental data satisfactorily when $\sigma > 4\Gamma/bL$ and demonstrates clearly that the rate of Coble creep can be slowed by more than an order of magnitude by the line tension of the dislocations when they act as imperfect sinks and sources for vacancies. The results are summarized in a deformation mechanism map in Fig. 8 which is conventional in that the fields occupied by Coble, Weertman and Harper–Dorn [27] creep are fields of fastest strain rate but unconventional in that the interface field is the field in which interface mechanisms are slower than Coble creep. The map gives the mechanisms which would be expected to be observed experimentally and it agrees well with all the experimental measurements on Sn alloys. The reason why values of m approaching 1 are not easily observed is that the diffusion-controlled Coble creep occupies only a narrow strip, typically only one decade in stress wide. On both sides of this strip are mechanisms with $m < 1$ and these mechanisms have a strong influence on the mechanical properties even in the centre of the Coble field. Pure Coble creep is only observed if the field is wider than about two decades in stress, i.e. if $(L/b) > 3 \times 10^5$.

The mechanism map, Fig. 8, is drawn for Sn at 298 K but the line separating Coble creep from interface-controlled creep is independent of

*A similar calculation for interface-controlled Herring–Nabarro creep also gives three terms with $\dot{\epsilon}_1 \propto \sigma/L^2$, $\dot{\epsilon}_2 \propto \sigma^2/L$, $\dot{\epsilon}_3 \propto \sigma^3$.

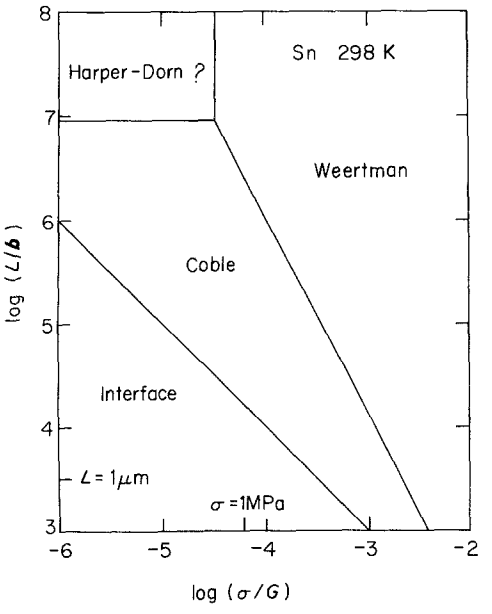

Figure 8 Mohamed–Langdon deformation mechanism map for Sn at 298 K. The line separating Coble creep from interface-controlled creep is independent of temperature and material.

material. It is worth noting that the transition observed in Al_2O_3 with $L = 1.2\,\mu m$ ($b = 0.48\,nm$) [35] between a low m behaviour at low stress and an m value of 1 at high stress ($> 30\,MPa$, $G = 1.3 \times 10^{11}\,Pa$) is in good agreement with the map.

Greenwood [36], using a dimensional argument based on the fact that when diffusion is interface-controlled the number of vacancies produced per second in a grain is proportional to the area of the grain face, showed that the strain rate is proportional to L^{-1}. If, in our model, $\dot{\epsilon}_2$ is the smallest component of $\dot{\epsilon}_d$ then $\dot{\epsilon} \propto L^{-2}$ in apparent disagreement with Greenwood. The reason for the discrepancy is that in our model the source of vacancies is a line rather than a plane.

5. Conclusions

(1) The occurrence of Coble creep has been established in Sn–2 wt% Pb by evaluating its plastic properties at room temperature and above, at a grain size of $\geqslant 50\,\mu m$ and a stress of ~ 1 MPa. It appears that the addition of Pb increases the GB self-diffusion coefficient in Sn by about one order of magnitude.

(2) Coble creep in Sn–2 wt% Pb is inhibited at low stresses, in particular for small grain sizes. The same applies probably also to Sn–38.1 wt% Pb. The inhibition is not caused by a threshold stress for plastic deformation.

(3) A model of Coble creep in which dislocation loops on the grain boundaries emit and absorb vacancies predict that Coble creep becomes interface-, rather than diffusion-controlled when $L\sigma/Gb < 1$, in good agreement with experiment in Sn–2 wt% Pb, Sn–38.1 wt% Pb and alumina.

(4) The observation that $\dot{\epsilon} \propto \sigma^2/L^2$ may be indicative of interface-controlled Coble creep and should not be taken as evidence that dislocations are climbing from the head of a pile-up.

Acknowledgements

The authors would like to thank Professor Sir Peter Hirsch for the provision of laboratory facilities and Dr R. C. Gifkins for his helpful comments on the manuscript. J. H. Schneibel acknowledges gratefully financial support by the German Academic Exchange Service and P. M. Hazzledine would like to thank the Chief and staff of CSIRO Division of Chemical Physics for their hospitality.

Appendix

Nabarro [10] proposed a dislocation creep model in which a mesh of dislocations, half of which are vacancy emitters and half vacancy absorbers, reaches a steady closest spacing of λ when the annihilation and creation rates are balanced. The model yields a strain rate, $\dot{\epsilon}$, which is proportional to σ^3. An equivalent model in two dimensions, corresponding to a net of dislocations on a grain boundary, gives the same result.

A square mesh of GB dislocations of side λ is assumed. Dislocations of opposite sign climb towards one another with a velocity v through their mutual attraction:

$$v = GbM/2\pi\lambda, \qquad \text{(A1)}$$

where M is the dislocation mobility (velocity/stress). Since the dislocations annihilate after a time λ/v, the annihilation rate is

$$(d\rho/dt) = -MGb/\pi\lambda^3, \qquad \text{(A2)}$$

if ρ is the dislocation density expressed as length per area of boundary. To balance this, dislocation loops grow under an effective stress, σ_e, which is the difference between the applied stress, σ_a, and the back stress from the line tension, Gb/λ. In a time interval $\lambda/M\sigma_e$, a loop of length $\sim 4\lambda$ is created by each source. The creation rate is, therefore,

$$(d\rho/dt) = 4M\sigma_e/\lambda^2. \qquad \text{(A3)}$$

In the steady state the sum of the creation and annihilation rates (Equations 2 and 3) is zero and the effective stress is, therefore,

$$\sigma_e = Gb/4\pi\lambda, \qquad \text{(A4)}$$

which is smaller than the applied stress σ by a factor of $(4\pi + 1)$. In the time interval $\lambda/\sigma_e M$, the boundary is swept by one dislocation, giving a strain increment of b/L; the strain rate is, therefore,

$$\dot{\epsilon} = Mb\sigma_e/L\lambda \sim Mb\sigma_a/4\pi L\lambda, \qquad \text{(A5)}$$

and since the mobility $M = 2wb^2D_B/kT\lambda$, the strain rate is

$$\dot{\epsilon} = b^3w\sigma_aD_B/2\pi L\lambda^2kT, \qquad \text{(A6)}$$

or, since $\sigma_a \simeq Gb/\lambda$, $\dot{\epsilon} \simeq (b/L)(\sigma/G)^3(GD_Bw/2\pi kT)$ which is of the same form as Equation 8, $\dot{\epsilon} \propto \sigma^3/L$.

References

1. R. L. COBLE, *J. Appl. Phys.* **34** (1963) 1679.
2. S. W. ZEHR and W. A. BACKOFEN, *Trans. ASM* **61** (1968) 300.
3. M. F. ASHBY and R. A. VERRALL, *Acta Metall.* **21** (1973) 149.
4. P. M. HAZZLEDINE and D. E. NEWBURY, *I.C.S.M.A. 3* **1** (1973) 202.
5. J. R. SPRINGARN and W. D. NIX, *Acta Metall.* **26** (1978) 1389.
6. J. W. EDINGTON, K. N. MELTON and C. P. CUTLER, *Prog. Mater. Sci.* **21** (1976) 61.
7. F. A. MOHAMED and T. G. LANGDON, *Phil. Mag.* **32** (1975) 697.
8. T. G. LANGDON and F. A. MOHAMED, *Scripta Metall.* **11** (1977) 575.
9. S. A. SHEI and T. G. LANGDON, *J. Mater. Sci.* **13** (1978) 1084.
10. F. R. N. NABARRO, *Phil. Mag.* **16** (1967) 231.
11. J. WEERTMAN, *Trans. ASM* **61** (1968) 681.
12. M. F. ASHBY, *Scripta Metall.* **3** (1969) 837.
13. *Idem, Surface Sci.* **31** (1972) 498.
14. R. C. GIFKINS, *Met. Trans.* **7A** (1976) 1225.
15. H. E. CLINE and T. H. ALDEN, *Trans. AIME* **239** (1967) 710.
16. P. M. HAZZLEDINE and D. E. NEWBURY, in "Grain Boundary Structure and Properties", edited by G. A. Chadwick and D. A. Smith (Academic Press, London, 1976) p. 235.
17. D. E. NEWBURY, D. Phil. Thesis, Oxford University (1972).
18. H. E. EXNER, *Int. Metall. Rev.* **17** (1972) 25.
19. J. E. BREEN and J. WEERTMAN, *Trans. AIME* **207** (1955) 1230.
20. T. H. ALDEN, *Acta Metall.* **15** (1967) 469.
21. B. BURTON, *Scripta Metall.* **5** (1971) 669.
22. A. E. GECKINLI and C. R. BARRETT, *ibid.* **8** (1974) 115.
23. J. H. SCHNEIBEL, *Acta Metall.* **28** (1980) 1527.
24. M. F. ASHBY, *I.C.S.M.A. 3* **2** (1973) 8.
25. G. SIMMONS and H. WANG, "Single Crystal Elastic Constants and Calculated Aggregate Properties: a Handbook" (M.I.T. Press, Cambridge, Mass., USA, 1971).
26. W. LANGE and D. BERGNER, *Phys. Stat. Sol.* **2** (1962) 1410.
27. F. A. MOHAMED, K. L. MURTY and J. W. MORRIS, *Met. Trans.* **4** (1973) 935.
28. C. HERRING, *J. Appl. Phys.* **21** (1950) 437.
29. J. P. STARK and W. R. UPTHEGROVE, *Trans. ASM* **59** (1966) 479.
30. B. BURTON, *Mater. Sci. Eng.* **10** (1972) 9.
31. C. M. F. RAE and D. A. SMITH, *Phil. Mag.* **A41** (1980) 477.
32. R. W. BALLUFFI, ASM Materials Science Seminar: "Grain Boundary Structure and Kinetics" (ASM, Metals Park, Ohio, 1979) p. 297.
33. T. G. LANGDON and F. A. MOHAMED, *J. Austral. Inst. Met.* **22** (1977) 189.
34. J. FRIEDEL, "Dislocations" (Pergamon Press, Oxford, 1964) p. 315.
35. R. M. CANNON, W. H. RHODES and A. H. HEUER, *J. Amer. Ceram. Soc.* **63** (1980) 46.
36. G. GREENWOOD, *Scripta Metall.* **4** (1970) 171.

Received 24 May
and accepted 16 July 1982